A R C H I V E S O F M E T A L L U R G Y A N D M A T E R I A L S
Volume 50 2005 Issue 3

K. KOWALCZYK-GAJEWSKA*, W. GAMBIN*, **, R.B. PĘCHERSKI*, ***,
J. OSTROWSKA-MACIEJEWSKA*

MODELING OF CRYSTALLOGRAPHIC TEXTURE DEVELOPMENT IN METALS ACCOUNTING FOR MICRO-SHEAR BANDS

MODELOWANIE ROZWOJU TEKSTURY KRYSTALOGRAFICZNEJ W METALACH Z UWZGLĘDNIENIEM MIKROPASM ŚCINANIA

The rigid-plastic model for the single grain is developed in which the velocity gradient is split into two parts connected with crystallographic slip and micro-shear bands respectively. For crystallographic slip the regularized Schmid law proposed by Gambin is used. For the micro-shear bands the model developed by Pęcherski, which accounts for the contribution of this mechanism in the rate of plastic deformation by means of a function f_{MS} is applied. Different constitutive equations for the plastic spin due to two considered mechanisms of plastic deformation are used. The presented model is applied to simulate crystallographic texture evolution in the polycrystalline element.

Opracowano sztywno-plastyczny model pojedynczego ziarna,w którym tensor gradientu prędkości został rozbity na dwie części związane odpowiednio z poślizgiem krystalograficznym i mikropasmami ścinania. Dla poślizgu krystalograficznego zastosowano regulryzowane prawo Schmida zaproponowane w pracy [8]. Dla mikropasm ścinania użyto formalizmu rozwiniętego w [18], gdzie uwzględnia się ich udział w przyroście deformacji plastycznej poprzez funkcję f_{MS}. Zastosowane zostały różne równania konstytutywne dla części spinu plastycznego wywołanych rozważanymi dwoma mechanizmami deformacji plastycznej. Zaprezentowany model wykorzystano w symulacji rozwoju tekstury krystalograficznej w elemencie polikrystalicznym.

* INSTITUTE OF FUNDAMENTAL TECHNOLOGICAL RESEARCH PAS, 00-049 WARSAW, ŚWIĘTOKRZYSKA 21, POLAND
** DEPARTMENT OF APPLIED MECHANICS, FACULTY OF MECHATRONICS, WARSAW UNIVERSITY OF TECHNOLOGY, 02-525 WARSAW, CHODKIEWICZA 8, POLAND
*** INSTITUTE OF STRUCTURAL MECHANICS, FACULTY OF CIVIL EUGINEERING, CRACOW UNIVERSITY OF TECHNOLOGY, WARSZAWSKA 24, 31-155 CRACOW, POLAND

1. Introduction

The mechanism of shear banding was studied in [19], where also the derivation of related macroscopic measure of the rate of deformation was presented. The continuum mechanics description of the kinematics due to shear banding made a basis for constitutive description proposed in [18, 20, 21, 22]. The attempts to identify the proposed model for simple case of symmetric shear banding occurring in the case of channel die test made possible to specify the contribution of shear banding as a logistic function of equivalent plastic strain [19], [16]. Such a function accounts for smooth increase of a contribution of micro-shear bands into the rate of plastic deformation, from zero for very small values of equivalent plastic strain to rapid growth within certain narrow strain interval up to the ultimate value, which is always lower than one.

1.1. Physical motivation

The available results of metallographic observations reveal that in heavily deformed metals, or even at small strains if they are preceded by a properly controlled change of deformation path, a multi-scale hierarchy of shear localization modes replaces the crystallographic multiple slip or twinning. Different terminology is used depending on the level of observation. In our study, the term micro-shear band is understood as a long and very thin (of order 0.1 mm) sheet-like region of concentrated and intensive plastic shear crossing grain boundaries without deviation and forming a definite pattern in relation to the principal directions of strain. The detail experimental information about mechanical behaviour and related structural features is reviewed in [18, 20, 21, 22] and [11, 12, 17], where also comprehensive lists of references are given. The clusters of micro-shear bands, produced for instance in rolling, form the planar structures, which are usually inclined by about $\pm 35°$ to the rolling plane and are orthogonal to the specimen lateral face. As it was already stressed in [18], it is typical of the clusters of active micro-shear bands that their planes are rotated relative to the respective planes of maximum shear stress by a certain angle β, which is usually of the order $(5 \div 15)°$. This is related with the important observation, discussed in [18], that a particular micro-shear band operates only once and develops fully in very short time. The micro-shear bands, once formed, do not contribute further to the increase in plastic shear strain. We assume that the successive generations of active micro-shear bands competing with the mechanism of multiple crystallographic slips are responsible for the process of advanced plastic flow.

1.2. General constitutive framework

Experimental observation confirm that micro-shear bands change the crystallographic texture evolution [9], [25] as well as the crystallographic texture of the polycrystal influences in the same time the initiation and development of micro-shear bands [2], [6].

There were many attempts to model shear banding phenomena. In [2] the polycrystalline aggregate composed of f.c.c. single grains was studied by FEM calculations. One element, being single crystal or a part of single crystal, was described by means of crystal plasticity model [4]. Shear bands in these calculations were identified as domains of concentrations of active crystallographic slip systems. Mutual correlation between the texture and shear banding identified in this way was found.

In some papers shear banding, mainly on the macro-scale but also on the micro-scale, is described as a result of material instability (instability of the constitutive equations) and connected to the strain localization phenomenon cf. review in [14]. It was proved that the strain localization of this kind could be achieved only with use of plasticity model with non-associated flow rule [24] or yield suvface with vertices without necessity to introduce the initial material inhomogeneity [15] or softening effect. In the case of crystal plasticity it led to the introduction of so-called non-Schmid effects to the constitutive equations [5]. However, describing of behavior of material in which the shear bands at macro-scale have already appeared requires non-standard, advanced calculation methods of post-critical analysis [23]. These methods seem to be not effective yet, to take into account micro-shear banding in large boundary value problems.

In this paper we propose another approach. Using the framework introduced in [18] we treat the micro-shear bands as the additional, mechanism of plastic deformation. In the model, according to the experimental observations, the contribution of this mechanism into the total rate of plastic deformation increases with the equivalent plastic strain and depends on the type of the deformation process. For the presented model the computational analysis of the prescribed boundary value problem may be performed with use of the standard algorithms established for the crystal plasticity theory.

Some drawback of the proposed method should be indicated comparing to the concurrent one. In the case of the proposed model some assumptions about the geometry of micro-shear bands with respect to the axes of strain and stress tensors must be made while in the instability analysis the geometry of micro-shear bands is one of the results of calculations. Let us note that the local microscopic strain and stress tensors are strictly connected with the local grain orientation and generally with texture evolution during the process. It seems that this is the source of the relation between the texture and micro-shear banding.

2. Kinematics

The rigid plastic model of single grain will be considered. In such a case for large strain formulation we use the following decomposition of the deformation gradient [3]

$$\mathbf{F} = \mathbf{F}^{*}\mathbf{F}^{p} = \mathbf{R}^{*}\mathbf{F}^{p}, \tag{2.1}$$

where $\mathbf{F}^* = \mathbf{R}^*$ is connected with the rigid rotation. Multiplicative decomposition of $\mathbf{F}$ results in additive decomposition of the total velocity gradient $\mathbf{L}$:

$$\mathbf{L} = \dot{\mathbf{F}}\mathbf{F}^{-1} = \underbrace{\dot{\mathbf{R}}^*\mathbf{R}^{*T}}_{\mathbf{L}^*} + \underbrace{\mathbf{R}^*\dot{\mathbf{F}}^p(\mathbf{F}^p)^{-1}\mathbf{R}^T}_{\mathbf{L}^p} \tag{2.2}$$

For the total velocity gradient we apply the decomposition into the symmetric part $\mathbf{D}$ (the strain rate tensor) and the skew-symmetric part $\boldsymbol{\Omega}$ (the spin tensor), that is

$$\mathbf{L} = \boldsymbol{\Omega} + \mathbf{D} = \boldsymbol{\Omega}^* + \boldsymbol{\Omega}^p + \mathbf{D}^p. \tag{2.3}$$

As it has been obtained above the rigid rotation part $\mathbf{L}^*$ is only skew-symmetric.

It is usually assumed that the crystallographic lattice is motionless in the course of plastic deformation and in rigid-plastic model is subjected only to the rigid rotation $\mathbf{R}^*$. Though, the lattice reorientation is described by $\boldsymbol{\Omega}^*$ in the form

$$\dot{\mathbf{a}} = \boldsymbol{\Omega}^*\mathbf{a}, \tag{2.4}$$

where $\mathbf{a}$ is some crystallographic direction in the current configuration of the single crystal.

One of the main assumptions of this paper, based on the derivation in [19], is that the plastic part $\mathbf{L}^p$ of the total velocity gradient may be decomposed into two parts

$$\mathbf{L}^p = \mathbf{L}^p_{slip} + \mathbf{L}^p_{MS}, \tag{2.5}$$

where $\mathbf{L}^p_{slip}$ is connected with the crystallographic slip mechanism of plastic deformation and $\mathbf{L}^p_{MS}$ with micro-shear bands. $\mathbf{L}^p_{slip}$ can be described as a sum of shearing on the active slip systems

$$\mathbf{L}^p_{slip} = \sum_{r=1}^{M} \dot{\gamma}^r \mathbf{m}_r \otimes \mathbf{n}_r, \tag{2.6}$$

where $\{\mathbf{m}_r, \mathbf{n}_r\}$ defines the slip system.

We assume also that micro-shear banding is due to double shear, so that [18]

$$\mathbf{L}^p_{MS} = \sum_{i=1}^{2} \dot{\gamma}^{(i)}_{SB} \mathbf{s}_i \otimes \mathbf{k}_i. \tag{2.7}$$

Moreover, it is assumed that two systems of micro-shear bands form the planar structure. It means that in some basis $\{\mathbf{e}_j\}$ for the current configuration of the body we obtain

$$\mathbf{s}_1 = \cos\phi\mathbf{e}_1 + \sin\phi\mathbf{e}_2, \qquad \mathbf{s}_2 = \cos\phi\mathbf{e}_1 - \sin\phi\mathbf{e}_2, \tag{2.8}$$

$$\mathbf{k}_1 = -\sin\phi\mathbf{e}_1 + \cos\phi\mathbf{e}_2, \qquad \mathbf{k}_2 = \sin\phi\mathbf{e}_1 + \cos\phi\mathbf{e}_2. \tag{2.9}$$

The directions $\{\mathbf{s}_i, \mathbf{k}_i\}$ depend on the actual strain tensor. The micro-shear band mechanism of plastic deformation is thought to be instantaneous what means that the geometry of bands in time t_1 can be completely different than that in time t_2. They should be established independently for subsequent deformation increments.

After the experimental observations it is postulated that $\{\mathbf{s}_i, \mathbf{k}_i\}$ are align with the prescribed angle to the principal directions of the strain tensor $\mathbf{E}^p$. In this case basis $\{\mathbf{e}_j\}$ is the basis of principal directions of strain tensor

$$\mathbf{E}^p = E_1^p \mathbf{e}_1 \otimes \mathbf{e}_1 + E_2^p \mathbf{e}_2 \otimes \mathbf{e}_2 + E_3^p \mathbf{e}_3 \otimes \mathbf{e}_3.$$

Further, let the bands be connected with the planes of the maximum shear strains. If $E_1 > E_3 > E_2$ then the situation presented in Figure 1 takes place and

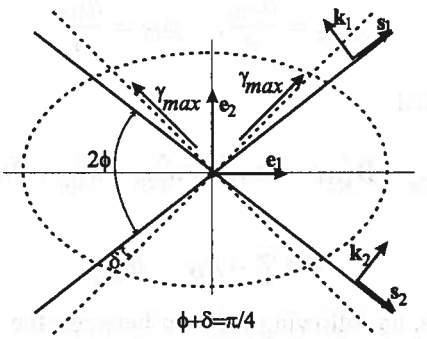

Fig. 1. Geometry of the planar structure of micro-shear bands

$$\gamma_{max} = |E_1^p - E_2^p|.$$

On the basis of the experimental observations one may approximate the angle $\delta \sim 5^\circ \div 10^\circ$ ($\phi \sim 38^\circ \pm 2^\circ$).

Using the decompositions (2.3) and (2.5) we obtain

$$\mathbf{D}^p = \mathbf{D}^p_{slip} + \mathbf{D}^p_{MS}, \tag{2.10}$$

$$\mathbf{\Omega}^p = \mathbf{\Omega}^p_{slip} + \mathbf{\Omega}^p_{MS} \tag{2.11}$$

and in view of (2.6) and (2.7)

$$\mathbf{D}^p_{slip} = \frac{1}{2} \sum_{r=1}^{M} \dot{\gamma}^r (\mathbf{m}_r \otimes \mathbf{n}_r + \mathbf{n}_r \otimes \mathbf{m}_r) = \sum_{r=1}^{M} \dot{\gamma}^r \mathbf{P}^r, \tag{2.12}$$

$$\mathbf{\Omega}^p_{slip} = \frac{1}{2} \sum_{r=1}^{M} \dot{\gamma}^r (\mathbf{m}_r \otimes \mathbf{n}_r - \mathbf{n}_r \otimes \mathbf{m}_r) = \sum_{r=1}^{M} \dot{\gamma}^r \mathbf{W}^r, \tag{2.13}$$

$$\mathbf{D}^p_{MS} = \frac{1}{2}\sum_{i=1}^{2}\dot{\gamma}^{(i)}_{SB}\left(\mathbf{s}_i \otimes \mathbf{k}_i + \mathbf{k}_i \otimes \mathbf{s}_i\right) = \sum_{i=1}^{2}\dot{\gamma}^{(i)}_{SB}\mathbf{N}^{(i)}, \tag{2.14}$$

$$\mathbf{\Omega}^p_{MS} = \frac{1}{2}\sum_{i=1}^{2}\dot{\gamma}^{(i)}_{SB}\left(\mathbf{s}_i \otimes \mathbf{k}_i - \mathbf{k}_i \otimes \mathbf{s}_i\right) = \sum_{i=1}^{2}\dot{\gamma}^{(i)}_{SB}\mathbf{S}^{(i)}. \tag{2.15}$$

Let us introduce the following notations for the magnitude of the considered strain rate tensors $\mathbf{D}^p$, $\mathbf{D}^p_{slip}$ and $\mathbf{D}^p_{MS}$ [1)]

$$\|\mathbf{D}^p\| = d, \quad \|\mathbf{D}^p_{slip}\| = d_{slip}, \quad \|\mathbf{D}^p_{MS}\| = d_{MS}$$

and denote as follows the ratios

$$f_{slip} = \frac{d_{slip}}{d}, \quad f_{MS} = \frac{d_{MS}}{d}. \tag{2.16}$$

Using (2.10) it is obtained

$$\|\mathbf{D}^p\| = \|\mathbf{D}^p_{slip} + \mathbf{D}^p_{MS}\| \Longleftrightarrow d^2 = d^2_{slip} + d^2_{MS} + 2d_{slip}d_{MS}\cos\Psi,$$

where

$$\cos\Psi = \boldsymbol{\mu}_{\mathbf{D}^p_{slip}} \cdot \boldsymbol{\mu}_{\mathbf{D}^p_{MS}}.$$

The above equality gives us following relation between the ratios

$$f^2_{slip} + f^2_{MS} + 2f_{slip}f_{MS}\cos\Psi = 1. \tag{2.17}$$

Additionally, for the strain rate tensor connected with the micro-shear bands we may calculate that

$$d^2_{MS} = \frac{1}{2}\left((\dot{\gamma}^{(1)}_{SB})^2 + (\dot{\gamma}^{(2)}_{SB})^2 + 2\dot{\gamma}^{(1)}_{SB}\dot{\gamma}^{(2)}_{SB}\cos 4\phi\right). \tag{2.18}$$

Similarly, introducing for the skew-symmetric part

$$\|\mathbf{\Omega}^p\| = \omega, \quad \|\mathbf{\Omega}^p_{slip}\| = \omega_{slip}, \quad \|\mathbf{\Omega}^p_{MS}\| = \omega_{MS}$$

and

$$\bar{f}_{slip} = \frac{\omega_{slip}}{\omega}, \quad \bar{f}_{MS} = \frac{\omega_{MS}}{\omega} \tag{2.19}$$

it is obtained

$$\bar{f}^2_{slip} + \bar{f}^2_{MS} + 2\bar{f}_{slip}\bar{f}_{MS}\cos\bar{\Psi} = 1, \tag{2.20}$$

[1)] Further in this paper the following notation will be used
$\|\mathbf{A}\| = \sqrt{\mathbf{A}\cdot\mathbf{A}} = \sqrt{A_{ij}A_{ij}}$, $\boldsymbol{\mu}_{\mathbf{A}} = \frac{\mathbf{A}}{\|\mathbf{A}\|}$,
where A is the second order tensor

where correspondingly

$$\cos\bar{\Psi} = \mu_{\Omega^p_{slip}} \cdot \mu_{\Omega^p_{MS}}.$$

For the micro-shear bands plastic spin we may calculate that

$$\omega^2_{MS} = \frac{1}{2}\left(\dot{\gamma}^{(1)}_{SB} + \dot{\gamma}^{(2)}_{SB}\right)^2. \tag{2.21}$$

3. Constitutive modelling

3.1. The regularized Schmid law and the constitutive equations for crystallographic slip

First, let us recall the single grain model with the regularized Schmid law [8, 13]. In view of this model the crystallographic slip mechanism is being given way when the following yield condition for the Cauchy stress σ is fulfilled

$$f(\sigma) = \frac{1}{2n}\sum_{r=1}^{M}\left(\frac{\tau^r}{\tau^r_c}\right)^{2n} - m = 0, \quad \tau^r = \mathbf{n}_r \cdot \sigma \cdot \mathbf{m}_r, \tag{3.1}$$

where τ^r_c is the critical value of the resolved shear stress on the slip system, n is the positive exponent and m is the material parameter independent of the lattice orientation [8].

The slip part of the strain rate tensor is associated to this yield condition

$$\mathbf{D}^p_{slip} = \dot{\lambda}\sum_{r=1}^{M}\frac{1}{\tau^r_c}\left(\frac{\tau^r}{\tau^r_c}\right)^{2n-1}\mathbf{P}^r \tag{3.2}$$

and for the plastic spin $\mathbf{\Omega}^p_{slip}$ we have

$$\mathbf{\Omega}^p_{slip} = \dot{\lambda}\sum_{r=1}^{M}\frac{1}{\tau^r_c}\left(\frac{\tau^r}{\tau^r_c}\right)^{2n-1}\mathbf{W}^r. \tag{3.3}$$

Comparing the above flow rules with the kinematic specifications (2.12) and (2.13) one may easily identify that

$$\dot{\gamma}^r = \dot{\lambda}\frac{1}{\tau^r_c}\left(\frac{\tau^r}{\tau^r_c}\right)^{2n-1}, \tag{3.4}$$

where $\dot{\lambda}$ is the plastic multiplier obtained in the classical way from the consistency condition $\dot{f} = 0$ or in the strain control processes from the current value of the magnitude of the strain rate tensor

$$\dot{\lambda} = \frac{df_{slip}}{\left\|\sum_{r=1}^{M}\frac{1}{\tau^r_c}\left(\frac{\tau^r}{\tau^r_c}\right)^{2n-1}\mathbf{P}^r\right\|}.$$

For the critical value of the resolved shear stress τ_c^r on the r^{th} slip system the hardening rule is usually postulated in the form

$$\dot{\tau}_c^r = \sum_{q=1}^{M} h_{rq}|\dot{\gamma}^q| \tag{3.5}$$

where h_{rq} are the components of the hardening moduli matrix. Different hardening rules were proposed in the literature. The most widely used are

- the Asaro rule [4]

$$h_{rq} = h(q + (1 - q)\delta_{rq})$$

in which h is the isotropic hardening function of the accumulated plastic strain ε_{eq}^p and q is the latent hardening ratio which takes values $1.1 \div 1.4$

- the W e n g rule [10]

$$h_{rq} = h(q + (1 - q)(\mathbf{m}_r \cdot \mathbf{m}_q)(\mathbf{n}_r \cdot \mathbf{n}_q))$$

in which h and q are defined as in the previous case but this formula, additionally, takes into account different hardening rates for co-planar and non co-planar slip systems.

Two constitutive models for the micro-shear bands mechanisms will be discussed below. In the first one the concept of non-associated plasticity is used. The second one is the simplified model developed analogically to one presented in [22].

3.2. Non-associated plasticity model for micro-shear bands

The yield condition (3.1) for the crystallographic slip mechanism in the presented model is in the same time the yield condition for the micro-shear bands mechanism. This statement corresponds to the experimental observation that micro-shearing is never activated without even small contribution of crystallographic slip.

Let us introduce two plastic potentials g_1 and g_2 for the double micro-shear mechanism. Using these potentials two components of the strain rate tensor $\mathbf{D}_{MS}^p$ can be derived as follows

$$\mathbf{D}_{MS}^{p(i)} = \dot{\lambda}^{(i)} \frac{\partial g_i}{\partial \boldsymbol{\sigma}}, \quad i = 1, 2.$$

In view of relation (2.14) it can be identified that

$$\boldsymbol{\mu}_{\frac{\partial g_i}{\partial \sigma}} = \sqrt{2}\mathbf{N}^{(i)}$$

and the simplest forms of potentials g_i analogous to the classical S c h m i d rule are

$$g_i(\boldsymbol{\sigma}) = \mathbf{N}^{(i)} \cdot \boldsymbol{\sigma}.$$

Further we assume the following relation

$$\frac{\dot{\lambda}^{(1)}}{\dot{\lambda}^{(2)}} = \frac{\dot{\gamma}^{(1)}_{SB}}{\dot{\gamma}^{(2)}_{SB}} = \frac{\mathbf{N}^{(1)} \cdot \boldsymbol{\sigma}}{\mathbf{N}^{(i)} \cdot \boldsymbol{\sigma}} = \eta. \tag{3.6}$$

Finally, it is obtained

$$\mathbf{D}^p_{MS} = \dot{\lambda}^{(1)}(\mathbf{N}^{(1)} + \eta\mathbf{N}^{(2)}) = \dot{\gamma}^{(1)}_{SB}(\mathbf{N}^{(1)} + \eta\mathbf{N}^{(2)}). \tag{3.7}$$

Introducing (3.7) into the relation (2.18) one arrives at

$$|\dot{\gamma}^{(1)}_{SB})| = \frac{\sqrt{2}}{\sqrt{1 + \eta^2 + 2\eta\cos 4\phi}} d_{MS}$$

The sign of $\dot{\gamma}^{(1)}_{SB}$ can be established from the condition of the positive plastic dissipation as the same as sign of the projection $\mathbf{N}^{(1)} \cdot \boldsymbol{\sigma}$. Eq. (3.7) can be rewritten in the form

$$\mathbf{D}^p_{MS} = df_{MS} \frac{\sqrt{2}\mathrm{sgn}(\mathbf{N}^{(1)} \cdot \boldsymbol{\sigma})}{\sqrt{1 + \eta^2 + 2\eta\cos 4\phi}} (\mathbf{N}^{(1)} + \eta\mathbf{N}^{(2)}). \tag{3.8}$$

It is worth noting that

$$\boldsymbol{\mu}_{\mathbf{D}^p_{MS}} = \mathrm{sgn}(\mathbf{N}^{(1)} \cdot \boldsymbol{\sigma}) \boldsymbol{\mu}_{\mathbf{N}^{(1)} + \eta\mathbf{N}^{(2)}}.$$

For the micro-shear band part of the plastic spin from Eq. (2.21) it is obtained

$$\omega_{MS} = df_{MS} \frac{|1 + \eta|}{\sqrt{1 + \eta^2 + 2\eta\cos 4\phi}} \tag{3.9}$$

and the part $\boldsymbol{\Omega}^p_{MS}$ of plastic spin can be calculated as

$$\boldsymbol{\Omega}^p_{MS} = df_{MS} \frac{\sqrt{2}\mathrm{sgn}(\mathbf{N}^{(1)} \cdot \boldsymbol{\sigma})}{\sqrt{1 + \eta^2 + 2\eta\cos 4\phi}} (\mathbf{S}^{(1)} + \eta\mathbf{S}^{(2)}). \tag{3.10}$$

At the end of this subsection let us formulate the above constitutive equations in the framework developed in the works concerning non-associated plasticity. According to this framework the tensor $\mathbf{D}^p_{MS}$ is decomposed into the part associated to the yield surface (3.1) (the regularized Schmid law) and the non-associated part. Let as introduce two IV-th order orthogonal projectors

$$\mathbb{I}_F = \boldsymbol{\mu}_{\frac{\partial f}{\partial \boldsymbol{\sigma}}} \otimes \boldsymbol{\mu}_{\frac{\partial f}{\partial \boldsymbol{\sigma}}}, \quad \mathbb{I}_T = \mathbb{I}_{dev} - \boldsymbol{\mu}_{\frac{\partial f}{\partial \boldsymbol{\sigma}}} \otimes \boldsymbol{\mu}_{\frac{\partial f}{\partial \boldsymbol{\sigma}}},$$

where $\mathbb{I}_{dev}$ is the tensor that projects into the space of deviatoric tensors

$$\mathbb{I}_{dev} = \mathbb{I} - \frac{1}{3}\mathbf{I} \otimes \mathbf{I}$$

and $\mathbb{I}$ and $\mathbf{I}$ are correspondingly the IVth order and IInd order identity tensors. The associated and non-associated components of $\mathbf{D}^p_{MS}$ are calculated as follows

$$\mathbf{D}^{p(a)}_{MS} = \mathbb{I}_F : \mathbf{D}^p_{MS} = (\boldsymbol{\mu}_{\frac{\partial f}{\partial \sigma}} \cdot \mathbf{D}^p_{MS})\boldsymbol{\mu}_{\frac{\partial f}{\partial \sigma}}, \tag{3.11}$$

$$\mathbf{D}^{p(na)}_{MS} = \mathbb{I}_T : \mathbf{D}^p_{MS} = \mathbf{D}^p_{MS} - \mathbf{D}^{p(a)}_{MS} = \|\mathbf{D}^{p(na)}_{MS}\|\boldsymbol{\mu}_T. \tag{3.12}$$

Using the notations introduced in Eqs (2.16) we may write

$$\mathbf{D}^p_{MS} = df_{MS}(\cos\Psi\boldsymbol{\mu}_{\frac{\partial f}{\partial \sigma}} + \sin\Psi\boldsymbol{\mu}_T). \tag{3.13}$$

According to the model presented above the angle Ψ is calculated as follows

$$\cos\Psi = \frac{\sqrt{2}\mathrm{sgn}(\mathbf{N}^{(1)} \cdot \boldsymbol{\sigma})}{\sqrt{1+\eta^2+2\eta\cos 4\phi}}(\mathbf{N}^{(1)} \cdot \boldsymbol{\mu}_{\frac{\partial f}{\partial \sigma}} + \eta\mathbf{N}^{(2)} \cdot \boldsymbol{\mu}_{\frac{\partial f}{\partial \sigma}}).$$

Let us note that in the above equations the significant role is played by the function f_{MS} that up to now remains not defined. We will come back to this issue later in this section.

3.3. The simplified model for micro-shear bands

In the simplified model for which the results of the simulations of crystallographic texture evolution are further presented we follow the concept presented in [16] for the H u b e r - M i s e s phenomenological model of plasticity. To simplify the constitutive modelling we assume that the strain rate tensor $\mathbf{D}^p_{MS}$ is associated to the yield surface described by Eq. (3.1). In such a case

$$\boldsymbol{\mu}_{\mathbf{D}^p_{MS}} \cdot \boldsymbol{\mu}_{\mathbf{D}^p_{slip}} = 1 \Longrightarrow \cos\Psi = 1. \tag{3.14}$$

Then, the constitutive equation has the simple form

$$\mathbf{D}^p = d(f_{slip} + f_{MS})\boldsymbol{\mu}_{\mathbf{D}^p_{slip}} = \frac{\dot{\lambda}}{1 - f_{MS}} \sum_{r=1}^{M} \frac{1}{\tau^r_c}\left(\frac{\tau^r}{\tau^r_c}\right)^{2n-1} \mathbf{P}^r. \tag{3.15}$$

The influence of micro-shear bands on the plastic yielding of the single grain is observed through the reduction of the hardening modules (3.5). In the presented model the hardening is solely due to crystallographic slip. Increasing contribution of micro-shear banding will cause reduction of the current value of the yield stress comparing to the model without micro-shear band mechanism of plastic deformation.

For the plastic spin $\boldsymbol{\Omega}^p_{MS}$ we follow the idea proposed by D a f a l i a s [7]. He connected the plastic spin with the non-coaxiality of the stress and strain rate tensors. In the discussed case this relation may be written as follows

$$\boldsymbol{\Omega}^p_{MS} = \zeta(\mathbf{D}^p_{MS}\boldsymbol{\sigma} - \boldsymbol{\sigma}\mathbf{D}^p_{MS}).$$

The above rule may be further rewritten in the form

$$\mathbf{\Omega}^p_{MS} = \omega \bar{f}_{MS} \mu_{\mathbf{D}^p_{MS}\sigma - \sigma \mathbf{D}^p_{MS}}.$$

Using the equation (2.19) it can be found that

$$\omega = \dot{\lambda} \frac{\| \sum_{r=1}^{M} \frac{1}{\tau_c^r} \left(\frac{\tau^r}{\tau_c^r} \right)^{2n-1} \mathbf{W}^r \|}{\bar{f}_{slip}}$$

and $\bar{f}_{slip}$ is related to $\bar{f}_{MS}$ through (2.20). The function $\bar{f}_{MS}$ is in the simplified model the additional unknown for which some constitutive equation should be supplied. In the simulations of texture development we have studied two cases

$$\bar{f}^I_{MS} = 0, \quad \bar{f}^{II}_{MS} = f_{MS}. \tag{3.16}$$

3.4. Definition of f_{MS} function

Now, let us pass to the definition of the f_{MS} function that describes the ratio of the plastic strain rate due to micro-shear banding in the total plastic strain rate. In [16] the process of constrained compression in channel die test was studied. For this process the following form of the f_{MS} function was assumed

$$f_{MS} = \frac{f^o_{MS}}{1 + \exp(a - b|\varepsilon|)}, \tag{3.17}$$

where material constants f^o_{MS}, a and b were identified for polycrystalline copper as $f^o_{MS} = 0.95$, $a = 7.5$, $b = 13.6$ and ε is the logarithmic strain in the compression direction in the considered process or in general a measure of equivalent plastic strain.

It is known from the experimental analysis that the imposed strain path as well as the change of this path during the process have the influence on the initiation and the development of the micro-shear bands. For example, in the uniaxial tension the contribution of this mechanism to the plastic deformation is rather small while in the channel die test this contribution is much more pronounced.

Constitutive modelling rules require the proposed function f_{MS} to be invariant with respect to the basis selection. The relation (3.17) does not take into account the influence of the plastic strain path on the micro-shear banding mechanism. Below, we would like to introduce the invariant form of this function that could be applied for any deformation process and accounts for the effect of the type of the strain path.

Let ξ be the some scalar function constructed with use of the invariants of the plastic part of strain tensor and the plastic strain rate tensor. Analogically to (3.17) let f_{MS} be of the logistic dependance of ξ so that

$$f_{MS}(\xi(\mathbf{E}^p, \mathbf{D}^p)) = \frac{f^o_{MS}}{1 + \exp(a - b\xi)}.$$

To fulfill the requirements imposed by the invoked experimental observations we recommend following ξ

$$\xi = \|\mathbf{E}^p\|(1 - \alpha|\cos 3\theta|), \quad 0 \leqslant \alpha \leqslant 1, \tag{3.18}$$

where

$$|\cos 3\theta| = 3\sqrt{6}|\det(\mu_{\mathbf{D}^p})|$$

and the coefficient α is an additional material parameter that describes the following ratio

$$\alpha = 1 - \frac{\xi_{\cos 3\theta=1}}{\xi_{\cos 3\theta=0}}$$

for the same value of the magnitude of the plastic strain for two extreme types of strain paths.

Let us note that for the proportional deformation path

$$\det(\mu_{\mathbf{D}^p}) = \det(\mu_{\mathbf{E}^p}) = const.$$

Fig. 2 presents f_{MS} given by Eq. (3.4) for the proportional deformation paths characterized by different values of the angle θ. The uniaxial, unconstrained tension

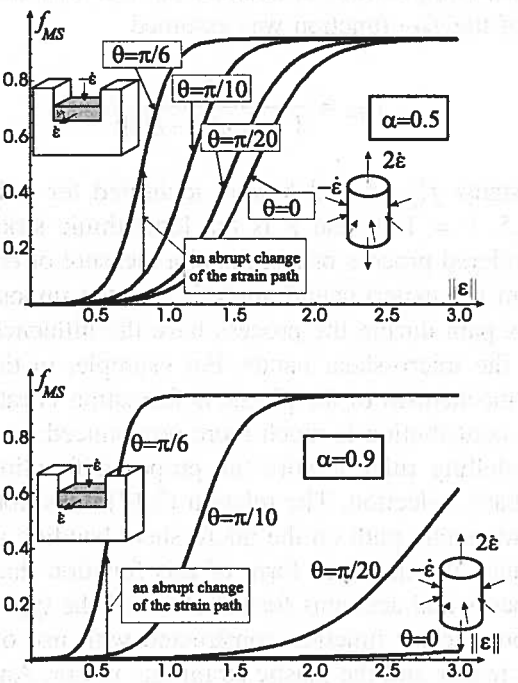

Fig. 2. The variation of f_{MS} representing contribution of micro-shear bands into the plastic strain rate in the course of the deformation process characterized by different proportional strain paths described by the angle θ

process gives $\theta = \pi/3$ while for the constrained plain strain process (the channel die test) $\theta = \pi/6$ is obtained. What happened for the presented model when the type of the proportional strain path is changed in the course of deformation process is schematically shown by the dashed line. In view of assumed f_{MS} in some cases rapid increase of the contribution of micro-shear bands may be observed. The shape of ξ function for some prescribed level of $\|\mathbf{E}^p\|$ is presented in Fig. 3. In figure function ξ is plotted in the deviatoric plane of the strain rate tensor for the proportional deformation path.

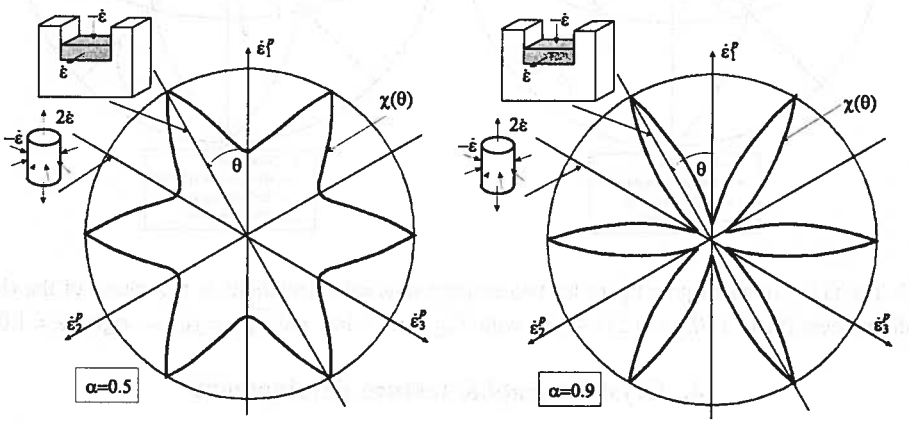

Fig. 3. The variation of ξ for the constant value of the equivalent plastic strain and different value of θ representing the type of the plastic strain path

Let us now show how the developed constitutive model predicts the lattice re-orientation during the process of large plastic deformations. We compare the results obtained for the classical model that does not incorporate the micro-shear bands as additional mechanism and two simplified models specified by (3.16) with micro-shear bands. For two arbitrary selected initial f.c.c. grain orientations we have performed calculations to obtain lattice rotation in the process similar to the channel die test. In Fig. 4 the standard pole figure (111) is presented for those orientations in the course of the deformation process for which the maximum contribution of micro-shear banding mechanism is predicted. The material parameters for copper cited in [1] were taken and additionally we have assumed $\alpha = 1.0$ in (3.18) and $n = 20$ in (3.1).

It can be observed that when the micro-shear banding is added the lattice orientation stabilizes earlier than for the model with pure crystallographic slip mechanism of plastic deformation. The difference between the models specified by (3.16) can be also noticed. In the first case the orientation path is preserved although the distance passed by the pole throughout the process is shorter comparing to the classical crystal plasticity model. In the second case, in the moment when the contribution of micro-shear banding becomes to be noticeable the orientation path starts to deviate from the path predicted by the classical model.

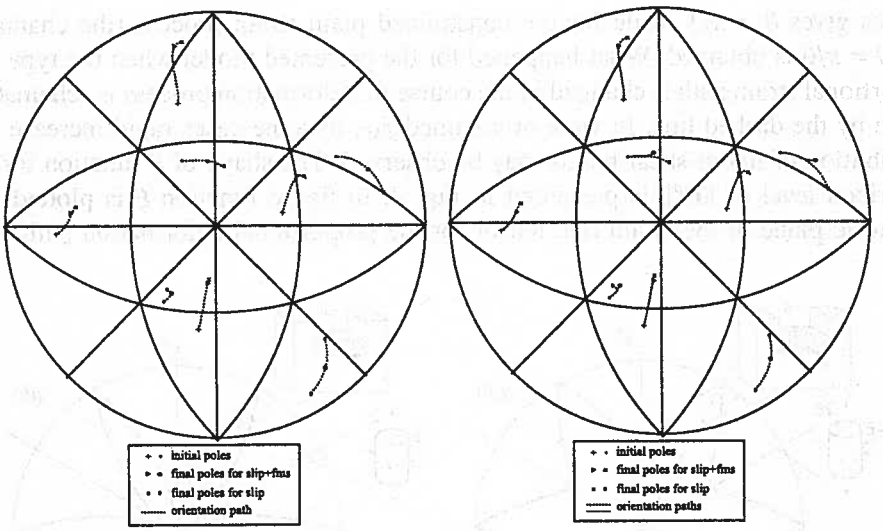

Fig. 4. The (111) standard pole figure for two arbitary selected orientations in the course of the channel die process (final: $L_3/L_3^0 = 0.25$) Model with $\overline{f}^{I}_{MS} = 0$ — left and $\overline{f}^{II}_{MS} = f_{MS}$ — right, $\alpha = 1.0$

4. Crystallographic texture development

The constitutive model accounting for two mechanisms of plastic deformation: crystallographic slip and micro-shear bands presented above was applied as a single grain model in the computations of the evolution of the crystallographic texture in the polycrystalline aggregate. Computations were conducted for the simplified model in which the plastic strain rates due to crystallographic slip and micro-shear banding are associated to the yield surface (3.1). Material parameters for copper were assumed similarly to the calculations discussed at the end of the previous section.

The classical Taylor assumption about equal velocity gradient $\mathbf{L}$ in every grain was taken. This assumption is equivalent to the statement that the field of velocity gradient is uniform within the aggregate.

In the calculated examples deviatoric, symmetric and uniform $\mathbf{L}$ and proportional paths of plastic strain were considered. Therefore, in the basis $\{\mathbf{e}_i\}$ of the main directions of the plastic strain tensor it is obtained

$$\mathbf{L} = \mathbf{D}^p \sim \dot{\varepsilon} \begin{pmatrix} l_1 & 0 & 0 \\ 0 & l_2 & 0 \\ 0 & 0 & -(l_1 + l_2) \end{pmatrix}, \quad \text{where} \quad l_i = const, \dot{\varepsilon} = const.$$

The $\dot{\varepsilon}$ is the constant in time plastic strain rate magnitude if we impose the following relation on l_i

$$l_1^2 + l_2^2 + (l_1 + l_2)^2 = 1.$$

Imposing initial condition on the deformation gradient $\mathbf{F} = \mathbf{I}$, boundary condition $\mathbf{v}(t)_{x_1=x_2=x_3=0} = 0$ and using the rules of continuum mechanics for large deformations one obtains the following representations of $\mathbf{F}(t)$ and the plastic strain rate tensor defined as $\mathbf{E}^p(t) = \ln \mathbf{V}(t) = \ln \sqrt{\mathbf{F}(t)\mathbf{F}^T(t)}$:

$$\mathbf{F}(t) \sim \begin{pmatrix} e^{\dot{\varepsilon} l_1 t} & 0 & 0 \\ 0 & e^{\dot{\varepsilon} l_2 t} & 0 \\ 0 & 0 & e^{-\dot{\varepsilon}(l_1+l_2)t} \end{pmatrix}, \quad \mathbf{E}^p(t) \sim \dot{\varepsilon} t \begin{pmatrix} l_1 & 0 & 0 \\ 0 & l_2 & 0 \\ 0 & 0 & -(l_1+l_2) \end{pmatrix} \tag{4.1}$$

In view of the above relations the current length of the material element in the direction $\mathbf{e}_i$ is given by

$$L_t^{(i)} = L_0^{(i)} e^{\dot{\varepsilon} l_i t} = L_0^{(i)} e^{E^p l_i},$$

where L_0 is the initial length of this material element and $E^p = \|\mathbf{E}^p\|$. Similarly the time t can be replaced by the magnitude of plastic strain tensor E^p in the relation (4.1). In the analyzed processes we obtain the following relation for the function ξ

$$\xi = E^p(1 - \alpha 3\sqrt{6}|l_1 l_2 (l_1 + l_2)|)$$

that linearly increases with time or equivalently with the plastic strain rate magnitude for the prescribed values of l_i.

In view of the above forms of $\mathbf{L}_p$, $\mathbf{E}^p$ and $\mathbf{F}$ and according to the relation (2.3) we obtain that

$$\mathbf{E}^p = \mathbf{E}^p_{MS} + \mathbf{E}^p_{slip} = (1 - f_{MS})\mathbf{E}^p + f_{MS}\mathbf{E}^p, \tag{4.2}$$

$$\mathbf{F} = \mathbf{F}_{MS}\mathbf{F}_{slip}. \tag{4.3}$$

It should be noted that the above decompositions are not so straightforward in the case of non-proportional strain path and in the model with non-associated flow rule for the micro-shear band part of the plastic strain rate tensor. However, if we assume the multi-

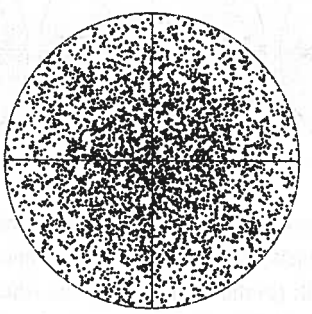

Fig. 5. The initial pole figure (111) for the polycrystalline aggregate

plicative decomposition (4.3) of the deformation gradient **F** the additive decomposition of **L** of the type (2.3) will result automatically.

Initial distribution of grain orientations within the aggregate was assume to be random. The initial crystallographic texture for the considered aggregate is presented in Fig. 5 in the form of the pole figure (111). Such a distribution of orientations results in initially isotropic properties of polycrystal on the macro-level.

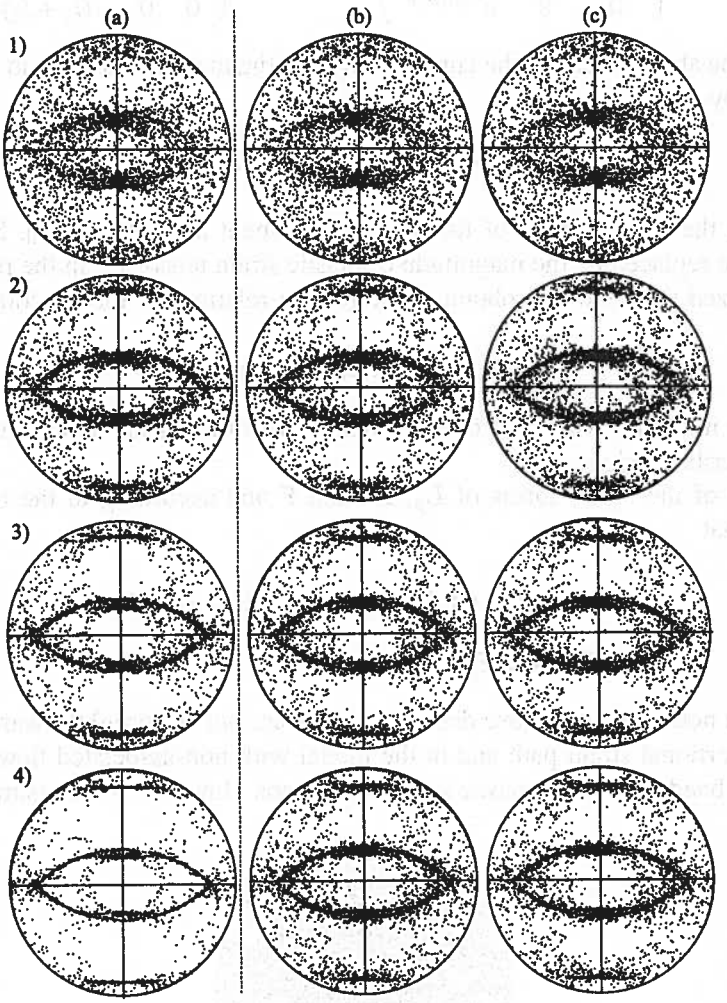

Fig. 6. The pole figures (111) in the course of the idealized channel-die process for the polycrystalline aggregate for three considered models: (a) the model without micro-shear bands; (b) the model with micro-shear bands and $\overline{f}^{I}_{MS} = 0$; (c) the model with micro-shear bands and $\overline{f}^{I}_{MS} = f_{MS}$ and 1) $L^{(3)}/L^{(3)}_0 = 0.757$, $f_{MS} = 0.022$; 2) $L^{(3)}/L^{(3)}_0 = 0.574$, $f_{MS} = 0.485$; 3) $L^{(3)}/L^{(3)}_0 = 0.435$, $f_{MS} = 0.929$; 4) $L^{(3)}/L^{(3)}_0 = 0.25$, $f_{MS} = 0.95$

Using computational program where the proposed model of single grain behavior was implemented the texture evolution was calculated for the ideal channel-die process. For this process $l_2 = 0$ and $l_1 = -l_3 = 1/\sqrt{2}$. The results of calculations are presented in Fig. 6 for three considered cases: the classical model without micro-shear bands and two variants of the proposed model specified by relations (3.16). As it is shown, initially, the texture evolves similarly for three models. After the f_{MS} reaches considerable value further increase of the contribution of micro-shear banding mechanism into the plastic deformation impedes the texture evolution. As a result the preferred orientation distribution predicted by the pure crystallographic slip model is not reached. The differences between two models given by (3.16) are secondary comparing to the effect described above and it is hard to notice them in the presented pole figures.

5. Conclusions and final remarks

In the paper the model of crystal plasticity accounting for additional mechanism of plastic deformation in the form of micro-shear banding has been proposed.

As a basis for the constitutive modelling the model with regularized S c h m i d law presented in [13] was assumed. Further, in order to incorporate the micro-shear banding into this model, the general framework proposed in [22] was adopted. In view of this framework the part of plastic strain rate due to micro-shearing was described by the non-associated flow rule. In the simplified model the contribution of micro-shear bands has been taken into account solely through its contribution function f_{MS} previously introduced for the classical H u b e r - M i s e s plasticity model [16].

In this paper the definition of f_{MS} was reformulated and proposed in the invariant form that takes into account the influence of the plastic strain rate path on the activation and development of the micro-shear bands mechanism. In the simplified model the influence of this mechanism is observed through the reduction of the hardening modules for the critical shear stress on the crystallographic slip system and by, in fact, "non-associated" rule for the plastic spin part attributed to the shear banding. This last feature of the model causes that the crystallographic texture development predicted by the proposed model different than that predicted by the pure crystallographic slip model. Generally, as it was shown in the previous section, due to large contribution of micro-shear banding into the plastic deformation the texture evolution is impeded and as a result the final texture for the same level of plastic strain magnitude is less pronounced than in the case of classical crystal plasticity.

In the calculations the T a y l o r model of polycrystalline aggregate was used. The assumption of this model about the same especially velocity gradient in every grain is very strong, in the presence of micro-shear bands. For the refined model with non-associated flow rule for $\mathbf{D}^p_{MS}$ part of plastic strain rate tensor this assumption should be modified in order to account for non-uniform plastic deformation field within the single grain and the aggregate. In order to develop such a model better understanding of geometry of micro-shear bands systems should be gained from experiments.

Acknowledgements

Most of the results reported in the paper were obtained in the framework of the research project No. 5 TO7A 031 22 supported by the State Committee for Scientific Research of Poland.

REFERENCES

[1] L. Anand, Single-crystal elasto-viscoplasticity: application to texture evolution in polycrystalline metals at large strain. Comput. Methods Appl. Mech. Engrg. **193**, 5359-5383 (2004).

[2] L. Anand, S.R. Kalidindi, The process of shear band formation in plane strain compression of fcc metals: Effects of crystallographic texture. Mech. Mater **17**, 223-243 (1994).

[3] R.J. Asaro, Crystal plasticity, J. Applied Mechanics **50**, 921-934 (1983).

[4] R.J. Asaro, A. Needleman. Texture development and strain hardening in rate depenedent polycrystals. Acta metall. **33**(6), 923- 953 (1985).

[5] R.J. Asero, J.R. Rice. Strain localization in ductile crystals. J. Mech. Phys. Solids **25**, 309-338 (1977).

[6] F. Basson, J.H. Driver. Deformation banding mechanisms during plane strain compression of cube-oriented f.c.c. crystals. Acta mater. **48**, 2101-2115 (2000).

[7] Y.F. Dafalias. Orientational evolution of plastic orthotropy in sheet metals. J. Mech. Phys. Solid **48**, 2231-2255 (2000).

[8] W. Gambin. Refined analysis of elastic-plastic crystals. Int. J. Solids Structures, **29**(16), 2013-2021 (1992).

[9] Z. Jasieński, J. Pospiech, A. Piątkowski, J. Kuśnierz, A. Litwora, K. Pawlik, H. Paul. Influence of shear banding on the texture in rolled and channel-die compressed polycrystalline copper. In Proc. of 10th ICOTOM, Material Science Forum, ed. H.J. Bunge, Trans. Tech. Publ. **157-162**, 1231-1237, 1994.

[10] A.S. Khan, P. Cheng. An anisotropic elactic-plastic constitutive model for single amd polycrystalline metals. I — theoretical developments. Int. J. Plasticity **12**, 147-162 (1996).

[11] A. Korbel. The mechanism of strain localization in metals. Arch. Metall. **35**, 177-203 (1990).

[12] A. Korbel. Structural and mechanical aspects of homogeneous and non-homogeneous deformation in solids, pages 21-98. Number 386. Udine 1997 in CISM Courses and LECTURES. Springer Wien New York, 1998.

[13] K. Kowalczyk, W. Gambin. Model of plastic anisotropy evolution with texture-dependent yield surface. Int. J. Plasticity **20**, 19-54 (2004).

[14] M. Li, O. Richmond. Intrinsic instability and nonuniformity of plastic deformation. Int. J. Plasticity **13**, 765-784 (1997).

[15] Z. Marciniak, K. Kuczyński. Limit strains in the processes of stretch-forming sheet metal. Int. J. Mech. Sci. 509 (1968).

[16] Z. Nowak, R.B. Pęcherski. Plastic strain in metals by shear banding. II. Numerical identification and verification of plastic flow accounting for shear banding. Arch. Mech. **54**, 621-634 (2002).

[17] H. Paul, Z. Jasieński, A. Piątkowski, A. Litwora, A. Pawełek. Crystallographic nature of shear bands in polycryslline copper. Arch. Metall. **41**, 337-353, 1996.

[18] R.B. Pęcherski. Modelling of large plastic deformation based the mechanism of micro-shear banding. Physical foundations and theoretical description in plane strain. Arch. Mech. **44**, 563-584 (1992).

[19] R.B. Pęcherski. Macroscopic measure of the rate deformation produced by micro-shear banding. Arch. Mech. **49**, 385-401 (1997).

[20] R.B. Pęcherski. Continuum mechanics description of plastic flow produced by micro-shear banding. Technische Mechanik **18**, 563-584 (1998).

[21] R.B. Pęcherski. Macroscopic effects of microshear banding in plasticity of metals. Acta Mechanica **131**, 203-224 (1998).

[22] R.B. Pęcherski, K. Korbel. Plastic strain in metals by shear banding. I. Constitutive description for simulation of metal shaping operations. Arch. Mech. **54**, 603-620 (2002).

[23] H. Petryk, K. Thermann. Post-critical deformation pattern in plane strain plastic flow with yield-surface vertex effect. Int. J. Mech. Sci. **42**, 2133-2146 (2000).

[24] J.W. Rudnicki, J.R. Rice. Conditions for the localization of deformation in pressure-sensitive dilatant materials. J. Mech. Phys. Solids **23**, 371 (1975).

[25] F. Stalony-Dobrzański, W. Bochniak. The role of micro-shear bands ithe formation of crystallographic texture in the deforming CuNi25. IV Seminarium Zintegrowane studia podstaw deformacji plastycznej metali, Nov 2004. In Pollish.

Received: 10 May 2005.